



HAL
open science

Measured and predicted of the longitudinal and transverse velocities of tube material using the Wigner-Ville and fuzzy logic techniques

Rachid Latif, Youssef Nahraoui, El Houcein Aassif, Gerard Maze

► To cite this version:

Rachid Latif, Youssef Nahraoui, El Houcein Aassif, Gerard Maze. Measured and predicted of the longitudinal and transverse velocities of tube material using the Wigner-Ville and fuzzy logic techniques. Acoustics 2012, Apr 2012, Nantes, France. hal-00810552

HAL Id: hal-00810552

<https://hal.science/hal-00810552>

Submitted on 23 Apr 2012

HAL is a multi-disciplinary open access archive for the deposit and dissemination of scientific research documents, whether they are published or not. The documents may come from teaching and research institutions in France or abroad, or from public or private research centers.

L'archive ouverte pluridisciplinaire **HAL**, est destinée au dépôt et à la diffusion de documents scientifiques de niveau recherche, publiés ou non, émanant des établissements d'enseignement et de recherche français ou étrangers, des laboratoires publics ou privés.



ACOUSTICS 2012

Measured and predicted of the longitudinal and transverse velocities of tube material using the Wigner-Ville and fuzzy logic techniques

R. Latif^a, Y. Nahraoui^a, E.H. Aassif^b and G. Maze^c

^aESSI ENSA Ibn Zohr University, ENSA BP 1136, 80000 Agadir, Morocco

^bFaculté des sciences d'Agadir, Université Ibn Zohr, Département de physique, Faculté des sciences d'Agadir, B.P 8106, 80000 Agadir, Morocco

^cLOMC, IUT, Université du Havre, Place Robert Schuman, Place Robert Schuman, 76610 Le Havre, France

latif_rachid@yahoo.fr

Intelligent modelling tools as artificial neural network and fuzzy logic approach are demonstrated to be competent when applied individually to a variety of problems such as modelling and prediction. Recently there has been a growing interest in combining both these approaches, and as a result, neuro-fuzzy (*ANFIS*) computing techniques have evolved. The advantage of using *ANFIS* for field modelling is given by the flexibility to adapt and relies on observed data rather than on analytical model of the system that some once it is difficult to establish it. The characterization of the material tube can be done through the longitudinal and transverse velocities of material tube. In this work, we applied the *ANFIS* for modelling and predicting of the cut-off frequency of the circumferential waves. The longitudinal and transverse velocities, of material tube, are determined from the predicted frequencies. The time-frequency (*SPWV*) and the proper modes theory (*PMT*) are used to compare and valid the values predicted by the *ANFIS*. The material density, the radius ratio b/a and the index i of the circumferential waves, are selected as the input parameters of the *ANFIS*. The useful data to train and to test the performances of the model are determined from the values obtained using the *PMT* and the *SPWV* techniques. The *SPWV* is representation is applied of the signal backscattered by an aluminium tube of radius ratio b/a (a : outer radius and b : inner radius) immersed in water. The *ANFIS* model is able to determine the longitudinal and transverse velocities of material tube, with a high precision of the different errors (*MRE*, *MAE*, *SE*). The obtained values of these velocities are in good agreement with those given in the scientific literature.

1 Introduction

Many studies, theoretical and experimental, show that acoustic resonances of a target are related to its physical and geometrical properties [1,3]. Conversely, starting from these resonances, we can characterize the material constituting a tube with a known geometry. If an air-filled tube immersed in water is excited by a plane acoustic wave perpendicularly to its axis, circumferential waves are generated in the shell and in the water/shell interface. For some frequencies, these circumferential waves form stationary waves on the circumference of the tube constituting resonances. The mode n of a resonance is the number of wavelengths around the circumference. These resonances are observed on the spectrum backscattered by a tube [3-5]. The circumferential waves can belong to two wave types which are equivalent to the Lamb waves on a plate: the antisymmetric (A_i) and symmetric (S_i) circumferential waves ($i = 1, 2$: wave index). For a material tube made of a , the resonance frequencies of these waves essentially depend on the radius ratio b/a . The modes of resonances n of a wave (A_i and S_i) line up on trajectories (n as function of the frequency). The characterization of the material constituting the tube can be done through the longitudinal and transverse velocities of material tube. In this work, we applied the *ANFIS* for modelling and predicting of cut-off frequency of the circumferential waves. The longitudinal and transverse velocities, of material tube, are determined from the predicted frequencies. The *PMT* and the *SPWV* techniques are used to compare these frequencies. The *SPWV* is applied of the acoustic signal, backscattered by an aluminium tube of $b/a=0,95$ is used for compare the results.

2 Acoustic scattering by a tube

The scattering of a plane wave by an infinite length tube with a radius ratio b/a is investigated through the solution of the wave equation and the associated boundary conditions. The figure 1 presents the mechanisms of the echo formation of the circumferential waves and the Scholte wave. The acoustic plane wave excited the tube normally to the z -axis. The fluid 2 filling the cavity of the shell has a density of ρ_2 and the velocity of longitudinal wave in this fluid is c_2 . In general, the outer fluid, labelled fluid 1, is different and its density is ρ_1 and the velocity of wave is c .

The pressure backscattered P_{scat} by a tube in a far field is the sum of the normal modes which takes into account the effects of the incident wave, the reflective wave ①, surface waves in the shell ② and interface Scholte wave ③ connected to the geometry of the tube. ② and ③ are the circumferential waves.

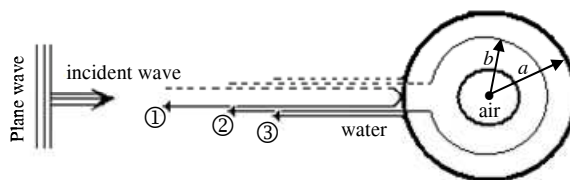


Figure 1: Mechanisms of the echo formation (①, ②, ③).

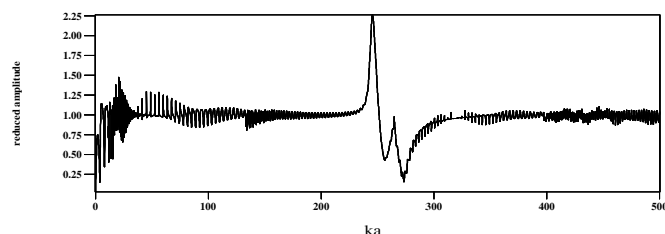


Figure 2: Backscattering spectrum of an air-filled aluminum tube immersed in water, $b/a = 0.95$.

The backscattered spectrum is given by [5]:

$$P_{scat}(\omega) = P_0 \sum_{n=0}^{\infty} \frac{D_n^{[1]}(\omega)}{D_n(\omega)} H_n^{(1)}(kr) \quad (1)$$

Where ω is the angular frequency, k is the wave-number, P_0 is the amplitude of the plane incident wave, $D_n^{[1]}(\omega)$ and $D_n(\omega)$ are determinants computed from the boundary conditions of the problem and $H_n^{(1)}(kr)$ is the Hankel function of the first kind.

P_{scat} is the backscattered spectrum computed in a far field. Figure 2 shows this spectrum as a function of the reduced frequency ka (without unit) given by:

$$ka = \frac{4\pi}{c(1-b/a)} f \frac{d}{2} \quad (2)$$

Where f is the frequency of a wave in Hz and d is the plate thickness ($d=a-b$).

The signal $P(t)$ of a tube is calculated by the inverse Fourier transform of the backscattered spectrum :

$$P(t) = \frac{1}{2\pi} \int_{-\infty}^{+\infty} h(\omega) P_{diff}(\omega) e^{-i\omega t} d\omega \quad (3)$$

Where $h(\omega)$ is a smoothing window.

Figure 3 shows the temporal signal backscattered by an aluminium tube with radii ratio $b/a=0.95$. This signal comprises a specular echo ① which one usually takes as origin of times. This echo is characterized by a short duration and a large amplitude. The specular echo is followed by a succession of elastic echoes of weak amplitudes. These amplitudes are spread out on a great duration ② and ③ which correspond to the circumferential waves ($S0, A1, S1, S2, A2, \dots$) and the Scholte wave (A). These different echoes end up overlapping and, in these conditions, their identification and arrival time measurements of these echoes become difficult, if not impossible. And is a major disadvantage of the temporal approach.

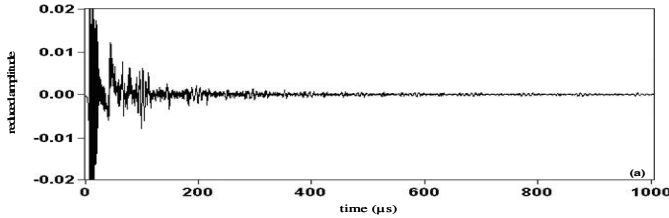


Figure 3: Temporal signal of an aluminum tube $b/a=0.95$.

The time-frequency technique, called Smoothed Pseudo Wigner-Ville ($SPWV$), is applied of the acoustic signal, backscattered by an aluminium tube of $b/a=0.95$. This $SPWV$ is given by [2, 4] :

$$SPWV_x(t, f) = \int_{-\infty}^{+\infty} \left| h\left(\frac{\tau}{2}\right) \right|^2 \int_{-\infty}^{+\infty} g(t-u) x\left(u + \frac{\tau}{2}\right) \times x^*\left(u - \frac{\tau}{2}\right) \exp(-2j\pi f\tau) dud\tau \quad (4)$$

The smoothing windows g and h are introduced into the $SPWV$ definition in order to allow a separate control of interferences either in time (g) or in frequency (h).

Figure 4 represents the $SPWV$ image for the anti-symmetric circumferential wave $A1$ for aluminium tube of $b/a=0.95$. On this time-frequency image we have noticed that the proper terms of the signal (circumferential waves) is well localised. And show synthetic image, from which can follow the evolution of the frequentiel content of the anti-symmetric wave $A1$ in time. For this $SPWV$ image the low frequencies part of the anti-symmetric wave $A1$ arrives more belatedly than high frequencies part. This means that the group velocity of this wave increases in function of frequency. When the time augments, the trajectory associated to anti-symmetric wave $A1$ tends to an asymptotic value which equals the cut-off frequency $(ka)_c$ of this wave. Using the proper modes theory, this frequency is calculated by [1, 3]. More precisely, this cut-off

frequency is the intersection point of the asymptotic trajectory of the anti-symmetric wave $A1$ and the axis of frequencies (figure 4). The values of the cut-off frequency $(ka)_c$ obtained from this image is presented in table 1. This table presents also those values computed with the proper modes theory (PMT). We notice that the cut-off frequencies determined from the $SPWV$ image are in good concordance with those computed from PMT .

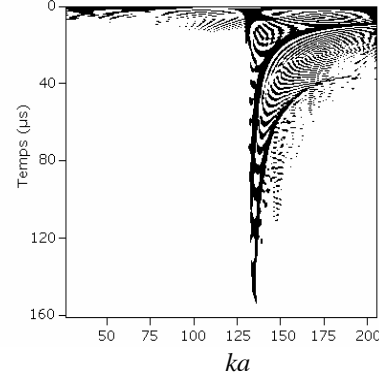


Figure 4: $SPWV$ of backscattered signal for aluminium tube.

3 ANFIS model

$ANFIS$ technique was originally presented by Jang [6-9]. For simplicity, we assume the fuzzy inference system with two input, x and y with one response f . From the first-order Sugeno fuzzy model, a typical rule set with two fuzzy if-then rules can expressed as below. The corresponding equivalent $ANFIS$ architecture is as shown in figure 5. The system architecture consists of five layers, namely; fuzzy layer, product layer, normalized layer, fuzzy layer and total output layer.

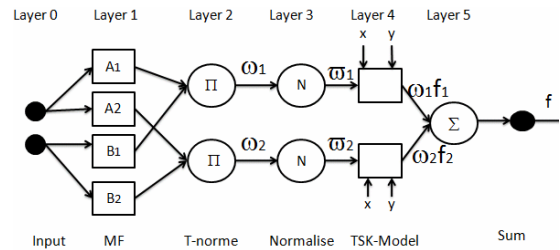


Figure 5: ANFIS architecture.

The following section in depth the relationship between the input and output of each layer in $ANFIS$.

Layer 0: It consists of plain input variable set.

Layer 1: It is the fuzzy layer. Each node in this layer generates a membership grade of a linguistic label. For instance, the node function of the i^{th} node may be generalized bell membership function:

$$\mu_{A_i} = 1 / (1 + [(x - c_i) / a_i]^b) \quad (5)$$

Where x is the input to node i ; A_i is the linguistic label associated with this node; and $\{a_i, b_i, c_i\}$ is the parameter set that changes the shapes of the membership function. Parameters in this layer are referred to as the premise parameters.

Layer 2: The function is T-norm operator that performs the firing strength of the rule. The simplest implementation just calculates the product of all incoming signals (Fig. 6).

$$\omega_i = \mu A_i(x) \mu B_i(y), \quad i=1,2 \quad (6)$$

Layer 3: Every node in this layer is fixed and determines a normalized firing strength. It calculates the ratio of the ratio of the j^{th} rule's firing strength to the sum of all rules firing strength.

$$\bar{\omega}_i = \omega_i / (\omega_1 + \omega_2), \quad i=1,2 \quad (7)$$

Layer 4: The nodes in this layer are adaptive are connected with the input nodes and the preceding node of layer 3. The result is the weighted output of the rule j .

$$\bar{\omega}_i f_i = \omega_i (p_i x + q_i y + r_i) \quad (8)$$

Where $\bar{\omega}_i$ is the output of layer 3 and $\{p_i, q_i, r_i\}$ is the parameter set. Parameters in this layer are referred to as the consequent parameters.

Layer 5: This layer consists of one single node which computes the overall output as the summation of all incoming signals.

$$\sum_i \bar{\omega}_i f_i = \sum_i \omega_i f_i / \sum_i \omega_i \quad (9)$$

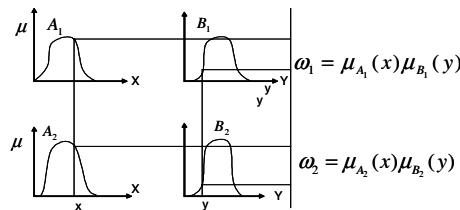


Figure 6: First-order Sugeno fuzzy model.

The basic learning rule of *ANFIS* is a combination of last square error and the back-propagation gradient descent, which calculates error signals recursively from the output layer backward to the input nodes. This learning rule is exactly the same as the back-propagation learning rule used in the common feed-forward neural networks. In this work, a data base is collected to involve and test the performance of the model starting from the results obtained by the PMT of the *AI* and *SI* waves. The density of material, the radius ratio, the index i of the *A* and *S* circumferential waves are retained like relevant entries of the model because these parameters characterize the tube and the types of circumferential waves. The transverse and longitudinal velocities of the *AI* and *SI* circumferential waves for a aluminium tube constitutes the output of *ANFIS*.

4 Velocities of material tube

Starting from the similarity which exists between the circumferential waves in the case of a thin tube and the Lamb waves in the case of a plate of a same thickness, it is possible to use the classical relations on the Lamb waves to determine the value of the cut-off frequency of the circumferential wave in the case of a tube [1, 3].

The cut-off frequencies of the circumferential waves in the case of a tube are given by [1, 3] :

$$(ka)_c^{\text{Symmetric}} = \frac{2\pi}{c(1-b/a)} \left\{ \frac{mc_T}{m + \frac{1}{2}} \right\} \quad (10)$$

$$(ka)_c^{\text{Antisymmetric}} = \frac{2\pi}{c(1-b/a)} \left\{ \frac{mc_L}{m + \frac{1}{2}} \right\} \quad (11)$$

Where c_L and c_T are longitudinal and transverse velocities of the tube respectively and m is the mode thickness (integer).

The expressions of the transverse c_T and the longitudinal c_L velocities, of the material constituting a tube, are determined from the relations of the cut-off frequencies of the *AI* and *SI* circumferential waves. The relations of these velocities are obtained respectively by :

$$c_T = \alpha \cdot (ka)_c^{\text{AI}} \quad (12)$$

$$c_L = \alpha \cdot (ka)_c^{\text{SI}} \quad (13)$$

Where $\alpha = c \cdot (1-b/a) / \pi$, $(ka)_c^{\text{AI}}$ and $(ka)_c^{\text{SI}}$ are the cut-off frequencies of the *AI* and *SI* waves.

5 Results and Discussion

The performance of *ANFIS* models for training and testing data sets were evaluated according to statistical criteria such as, coefficient of correlation R , *MAE*, *MRE*, *SE*, and Root Mean Square Error (*RMSE*). The selection of different models is done comparing the errors of the *ANFIS* configuration, calculating the *MAE*, the *MRE* and the *SE* of the cut-off frequencies. The coefficient of correlation R and the determination R^2 of the linear regression are used like performance measures of the model between the predicted and the desired output. The different error measures and the coefficient of correlation are given by the following relations:

$$MAE = \frac{1}{n} \sum_{i=1}^n |D_i - P_i| \quad (14)$$

$$MRE = \frac{1}{n} \sum_{i=1}^n \frac{|D_i - P_i|}{D_i} \quad (15)$$

$$R = 1 - \frac{\sum_{i=1}^n (D_i - P_i)^2}{\sum_{i=1}^n (D_i - P_m)^2} \quad (16)$$

$$SE = \sqrt{\frac{\sum_{i=1}^n (D_i - P_i)^2}{n-1}} \quad (17)$$

Where n is the number of data, P_i and D_i is the predicted and desired of cut-off frequencies respectively and P_m is the mean of predicted values.

The coefficient of correlation is a commonly used statistic and provides information on the strength of linear relationship between the observed and the computed values. The training and testing performances of *ANFIS* models are given in figures 7 to 9. The analysis is repeated several times. Indeed, the error values are measured for each *ANFIS* architecture based on the number of rules and the type of the membership function used. In this work we tried to play on the number of rules and the number of epochs we have observed that the error values of our model decrease more than the number of rules, and the number of epochs is increases. The results are presented in figures 7 to 9 for each circumferential wave (*A1*, *S1*) for aluminium tube with $b/a=0,95$. The figures show that the results obtained by the *ANFIS* method are in good agreement with those determined from the results calculated using the *PMT*.

The values of the cut-off frequencies $(ka)_c$ of the *A1* and *S1* waves obtained by the *ANFIS* model, the *SPWV* and the *PMT* (relations (10) and (11)) for the aluminium tube of $b/a=0,95$ are provided in table 1. From the results of figures 6 to 8, the model is able to predict the cut-off frequencies of the *S1* and the *A1* waves, with a high precision (Table 2) of the different errors (*MRE*, *MAE*, *SE*). A good agreement is obtained between the output values predicted using the propose model and those computed by the *PMT* and *SPWV*.

Table 1: Results of the cut-off frequency of *A1* and *S1*.

Mode	PMT	ANFIS	SPWV
A1	132.5	132,49	131
S1	265.0	271,2	266

Table 2: Results of the different error measures.

Error	Mode <i>A1</i>	Mode <i>S1</i>
MAE	0.03 ka	0.08 ka
MRE	$0.8 \cdot 10^{-3}$ ka	$0.8 \cdot 10^{-3}$ ka
SE	$9 \cdot 10^{-3}$ ka	10^{-2} ka
$R=R^2$	1	1

The cut-off frequencies values of the *A1* and *S1* waves are determined from the *SPWV*, the *PMT* and the *ANFIS* and given in tables 3 and 4. From these values we have determined with precision the transverse and the longitudinal velocities of aluminium material tube using the equations (12) and (13). The results obtained are illustrated in table 3 for *A1* and in table 4 for *S1*. The experimental values of the transverse and the longitudinal velocities, given in the scientific literature, are also included in the same table.

A good agreement is noted between the results obtained from the different methods. According to the results illustrated in tables 3 and 4, we observed that the estimation

errors from the *ANFIS* model do not exceed 1 %. However, we have determined with precision the longitudinal and the transverse velocities values of the material constituting a tube.

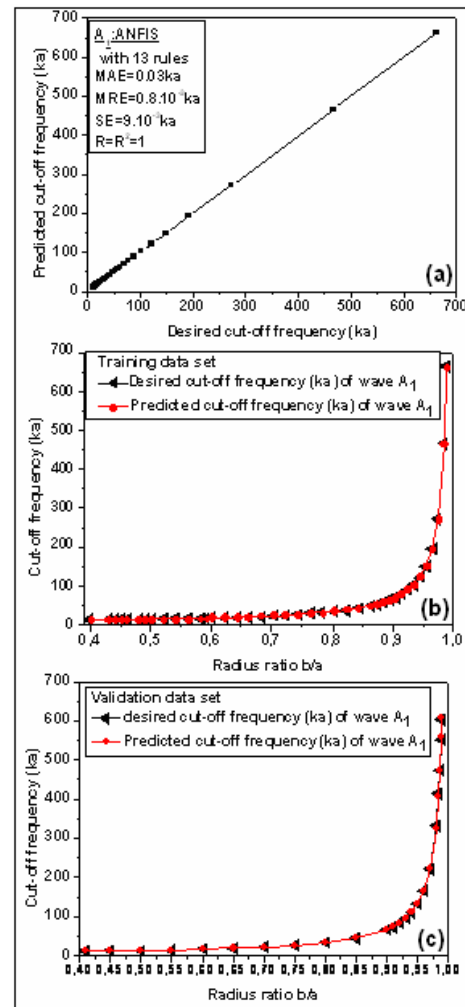


Figure 7: Results of *ANFIS* model for *A1*.

Table 3: Results of C_T (^{SL}: Scientific Literature).

	SPWV	PMT	ANFIS
$(ka)_c$	131 ± 0.3	132.5	132,49
C_T (m/s)	3090 ± 14	3111	3101,27
C_T (m/s) ^{SL}	3100		

Table 4: Results of C_L .

	SPWV	PMT	ANFIS
$(ka)_c$	266 ± 0.3	265.0	271,2
C_L (m/s)	6457 ± 14	6312.5	6348,15
C_L (m/s) ^{SL}	6380		

5 Conclusion

The main aim of this work was to train an *ANFIS* to predict cut-off frequency with the minimum of input data. Results show that the trained model can be used as an alternative way in the modelling behaviour system. This

ANFIS taking into account some characteristics of the tube is developed in order to predict the cut-off frequency of A_1 and S_1 circumferential waves. This method allows one to determine automatically and with good precision the cut-off frequency of the circumferential waves. The longitudinal and transverse velocities of material tube are determined with a high precision from the cut-off frequencies predicted with the *ANFIS* model. The R^2 value is about 1, which can be considered as very satisfactory. The obtained values of the longitudinal and transverse velocities of material tube are in good agreement with those given in the scientific literature.

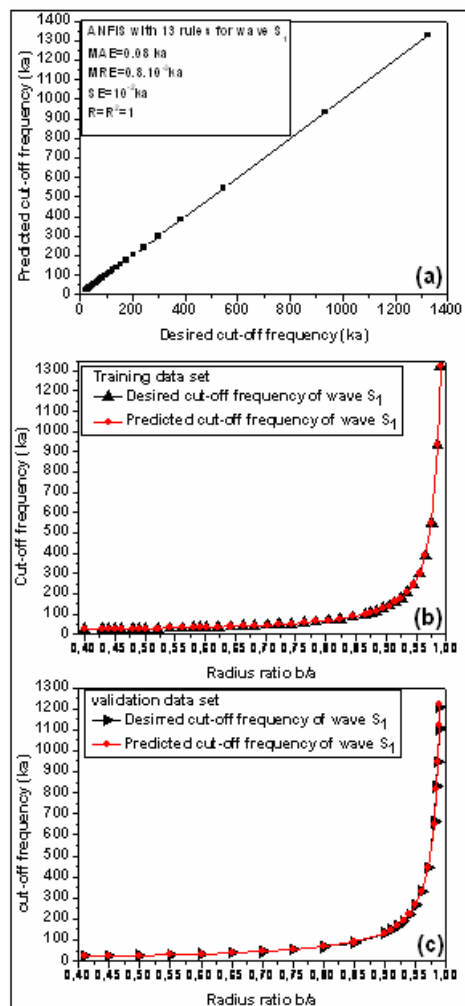


Figure 8: Results of *ANFIS* model for S_1 .

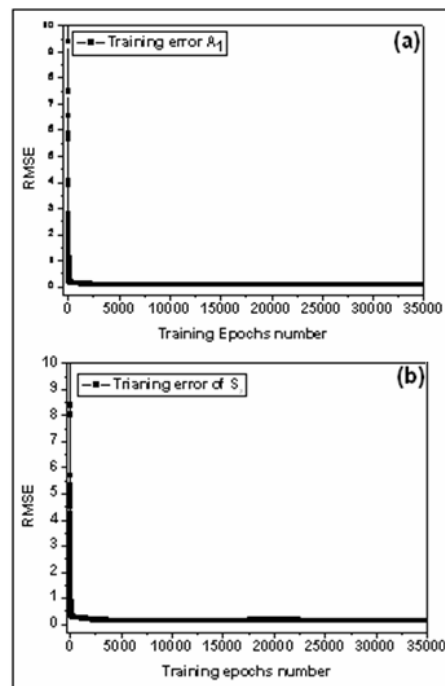


Figure 9: Errors of training and testing of A_1 (a) and S_1 (b).

References

- [1] R. Latif, E. Aassif, A. Moudden, D. Decultot, B. Faiz, and G. Maze, "Determination of the cut-off frequency of an acoustic circumferential wave using a time-frequency analysis," *J. NDT&E Int.*, vol. 33, pp. 373–376, (2000)
- [2] M. Talmant, J. L. Izbicki, G. Maze, G. Quentin J. Ripoche. "External wave resonance on thin cylindrical shells". *J. Acoustique*, 4, pp. 509-523, (1991)
- [3] R. Latif, E. Aassif, M. Laaboubi, G. Maze, "Détermination de l'épaisseur d'un tube élastique à partir de l'analyse temps-fréquence de Wigner-Ville", *Acta Acustica united with Acustica*, Vol. 95, pp. 253-257, (2009)
- [4] P. L. Marston and N. H. Sun, "Backscattering near the coincidence frequency of a thin cylindrical shell: Surface wave properties from elastic theory and an approximate ray synthesis," *J. Acoust. Soc. Amer.*, vol. 97, pp. 777–783, (1995)
- [5] G. Maze, "Acoustic scattering from submerged cylinders. MIIR Im/Re: Experimental and theoretical study," *J. Acoust. Soc. Amer.*, vol. 89, pp. 2559–2566, (1991)
- [6] Jang J-SR. *ANFIS: Adaptive-network-based fuzzy inference systems*. *IEEE Trans Syst Man Cybern*, 23(3), pp. 665–85, (1993)
- [7] H. Ishibuchi, R. Fujioka, and H. Tanaka. *IEEE Trans. Fuzzy Systems* 1, pp. 85-97, (1993)
- [8] Lee CC. *Fuzzy logic in control system: Fuzzy logic controller—part I and part II*. *IEEE Trans Syst Man Cybern*, 20(2), pp. 404–35, (1990)
- [9] Sugeno M. *Industrial applications of fuzzy control*. New York: Elsevier Ltd., (1985)